Proc. Natl. Acad. Sci. USA
Vol. 87, pp. 1668–1672, March 1990
Biochemistry

Substrate sequence effects on "hammerhead" RNA catalytic efficiency

(RNA secondary structure/antisense RNA/RNA enzymes)

MARTHA J. FEDOR AND OLKE C. UHLENBECK*

Department of Chemistry and Biochemistry, Campus Box 215, University of Colorado, Boulder, CO 80309-0215

Communicated by Thomas R. Cech, December 4, 1989

ABSTRACT **The "hammerhead" RNA self-cleaving domain can be assembled from two RNA molecules: a large (≈34 nucleotide) ribozyme RNA containing most of the catalytically essential nucleotides and a small (≈13 nucleotide) substrate RNA containing the cleavage site. Four such hammerheads that contained identical catalytic core sequences but differed in the base composition of the helices that are involved in substrate binding had been reported to vary in cleavage rates by more than 70-fold under similar reaction conditions. Steady-state kinetic analyses reveal that k_{cat} values are nearly the same for these hammerheads but K_m values vary nearly 60-fold. The substrates for reactions having high K_m values form aggregates that are virtually nonreactive. These observations demonstrate that the secondary structure of substrate RNA can be a major determinant of hammerhead catalytic efficiency.**

The RNA genomes of certain plant viroids and virusoids were discovered to be capable of spontaneous cleavage at a unique location in a reaction that generates monomeric genomes following rolling circle replication (1–3). Comparison of several self-cleaving RNA sequences led to the identification of a consensus secondary structure, termed the "hammerhead," containing 11 conserved nucleotides at the junction of three helices that are precisely positioned with respect to the cleavage site (4). A hammerhead of <60 contiguous nucleotides was found to be sufficient for rapid cleavage in the absence of protein (5–7). Although the hammerhead is normally formed from sequences within a single molecule, it can be assembled from two RNA molecules of approximately equal size that associate by base pairing (8). The domain can also be assembled from a larger ribozyme RNA containing most of the conserved nucleotides and a small substrate RNA containing the cleavage site (9–11). Hammerhead domains of this latter type have been designed so that the ribozyme associates with a larger target RNA to cleave a specific sequence, acting in a fashion analogous to DNA restriction endonucleases (9, 11).

Four hammerhead sequences were found to cleave at velocities that varied over 70-fold under similar reaction conditions (10). These hammerheads contained all the conserved nucleotides but differed in the sequence of the intermolecular helices formed upon substrate binding. Here we examine the kinetics of cleavage for several hammerhead sequences to characterize the reaction mechanism and explore how nucleotides involved in substrate binding affect cleavage. Results of these experiments led us to evaluate how secondary structures of hammerhead constituents influence reaction kinetics. Understanding the constraints imposed on hammerhead catalysis by helix base composition should assist in the design of ribozymes employed as endonucleases for the cleavage of specific target RNAs (9, 11).

The publication costs of this article were defrayed in part by page charge payment. This article must therefore be hereby marked "*advertisement*" in accordance with 18 U.S.C. §1734 solely to indicate this fact.

MATERIALS AND METHODS

RNA was synthesized by T7 RNA polymerase transcription of partially duplex synthetic DNA templates (12). For transcription of radiolabeled RNA (12–36 Ci/mmol; 1 Ci = 37 GBq), a typical 50-μl reaction contained 40 mM Tris Cl (pH 8.1), 1 mM $MgCl_2$, 1 mM spermidine, 5 mM dithiothreitol, 0.01% Triton X-100, 0.2 μM template, T7 RNA polymerase at 0.1 mg/ml, and three NTPs (each at 1 mM). The concentration of the fourth NTP was reduced to 0.2 mM and combined with 350 μCi of the corresponding [α-^{32}P]NTP (≈3000 Ci/mmol). For transcription of nonradiolabeled RNA, NTP concentrations were elevated to 2 mM or 4 mM, and the concentration of $MgCl_2$ was increased to 25 mM. Transcription reactions were carried out at 37°C for 1 hr for radiolabeled RNA and 3 hr for nonradiolabeled RNA. Transcription reactions were fractionated by using acrylamide gels containing 7 M urea. Products were located by autoradiography or UV shadowing, eluted in 0.25 M ammonium acetate/10 mM Tris Cl, pH 7.9/1 mM EDTA, and then concentrated by DEAE chromatography and ethanol precipitation. RNA was dissolved in 50 mM Tris Cl (pH 7.5) and stored at −20°C. 5′-^{32}P-labeled RNA (3600 Ci/mmol) was prepared by treatment with bovine alkaline phosphatase followed by reaction with T4 polynucleotide kinase and [γ-^{32}P]ATP (6000 Ci/mmol). Concentrations were determined by assuming a residue extinction coefficient at 260 nm of 6.6×10^3 $M^{-1} \cdot cm^{-1}$.

Because most transcription reactions generate multiple products that are smaller or larger than the desired oligonucleotide, care was taken to identify the correct transcript. The correct 3′ terminal nucleotide was verified for ribozymes and substrates of hammerheads 6 and 10 by complete RNase digestion of [5′-^{32}P]pCp 3′-end-labeled material (13) and two-dimensional PEI-cellulose TLC with appropriate standards (14). Substrates of hammerheads 6 and 10 were also sequenced by partial enzymatic hydrolysis. The remaining RNAs were identified by coelectrophoresis on denaturing gels with completely characterized markers.

To disrupt aggregation states potentially formed during RNA storage (15), solutions of both the ribozyme RNA and the combined radiolabeled and nonradiolabeled substrate RNAs were heated separately in 50 mM Tris Cl (pH 7.5) at 95°C for 1 min and allowed to cool to the reaction temperature of 25°C. Each RNA solution was then adjusted to a final concentration of 10 mM $MgCl_2$ and allowed to incubate at 25°C for 15 min. This procedure was adopted because failure to preincubate in magnesium led to anomalous initial rates. Cleavage reactions were initiated by adding the ribozyme to the substrate. Samples were removed at intervals, quenched with an equal volume of 7 M urea/50 mM EDTA/0.04% bromophenol blue/0.04% xylene cyanol/5 μM carrier oligoribonucleotide, and then fractionated by electrophoresis into 20% acrylamide/7 M urea gels. Substrate and product bands

*To whom reprint requests should be addressed.

were located by autoradiography, excised, and counted to determine the fraction of cleavage. For determination of k_{cat} and K_m values, steady-state rates were measured with at least seven substrate concentrations and one or more concentrations of ribozyme. Values of k_{cat} and K_m determined from duplicate experiments using Eadie–Hofstee plots (16, 17) showed <30% variation.

Nondenaturing gel electrophoresis was carried out using 15% acrylamide (acrylamide/bisacrylamide, 19:1) gels (25 × 15 × 0.15 cm) in 50 mM Tris acetate, pH 7.5/10 mM magnesium acetate buffer at room temperature. Radiolabeled and nonradiolabeled RNAs were combined in 50 mM Tris Cl (pH 7.5), heated to 95°C for 1 min, and allowed to cool to room temperature. Glycerol was then added to a final concentration of 5%. Electrophoresis was at 11 W for 14 hr following a 2-hr period of preelectrophoresis at 20 W.

RESULTS

The four hammerhead sequences in Fig. 1 are composed of a large RNA, or ribozyme, containing most of the nucleotides thought to comprise the catalytic core and a small substrate RNA containing the cleavage site. These hammerheads contain the same nucleotides at the junction of the helices but differ in the sequence of the intermolecular helices generated by substrate binding. A minimal hammerhead reaction mechanism includes assembly and catalysis followed by the exchange of cleavage products for intact substrate. *A priori*, the effect of helix base composition of hammerhead catalytic efficiency might result from an influence on K_d, the rate of cleavage chemistry, or the rate of product dissociation.

Cleavage rates were measured during the first few turnovers to help identify which step in the cleavage mechanism might be rate-determining and to define conditions appropriate for steady-state measurements (Fig. 2). A lag in the initial turnover might indicate a requirement for a slow conformational change upon substrate binding before accumulation of an active hammerhead complex. A rapid initial turnover might indicate that product dissociation was rate-determining. For hammerheads 8 and 9, no rate inflections were observed during the approach to steady state. Rates extrapolate to zero product at zero time, ruling out a significant "burst" of product formation. For hammerheads 6 and 10, however, a small rate decrease of <2-fold occurs early in the course of cleavage, and plots of steady-state rates extrapolate to amounts of product greater than zero at zero time. This could reflect a low rate of product dissociation relative to earlier steps in the reaction, but alternative explanations, such as the slow formation of a nonproductive ribozyme–substrate complex, have not been ruled out. Although the differences between initial and steady-state rates are small, care was taken to collect data during the true steady-state phase of the cleavage reaction for the determination of Michaelis–Menten parameters. These experiments also serve to demonstrate that cleavage is clearly catalytic, with multiple cycles of catalysis generating many molar equivalents of product relative to ribozyme.

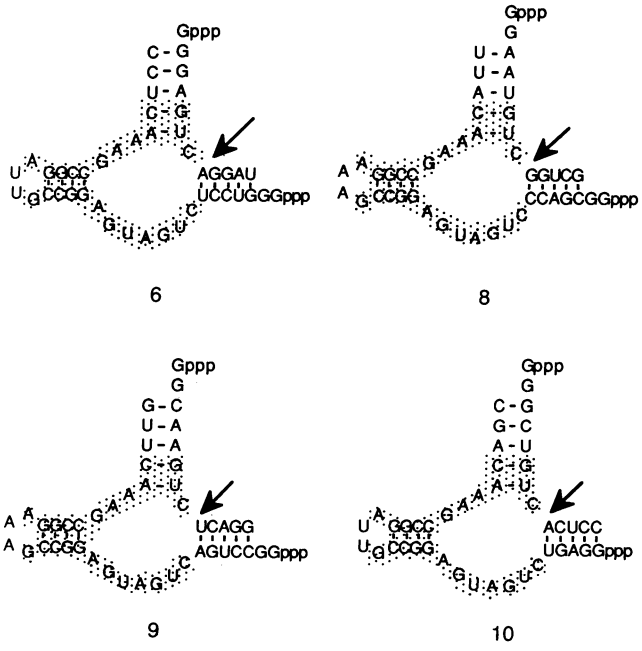

FIG. 1. Four hammerhead domain sequences. Stippled nucleotides are identical among the hammerhead domains. Arrows indicate the sites of cleavage.

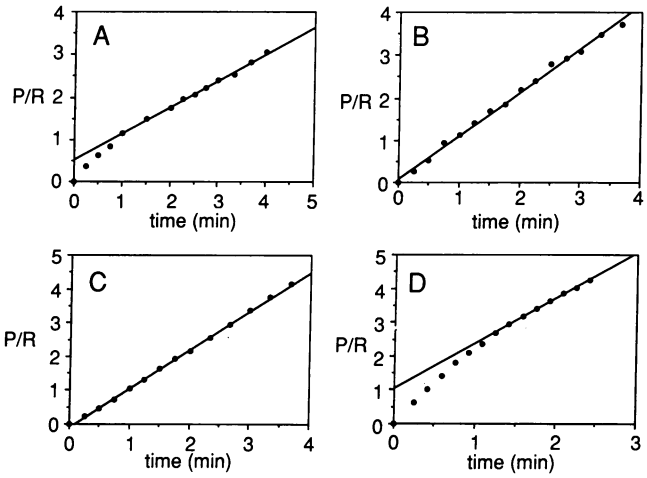

FIG. 2. Hammerhead kinetics during the approach to steady state. The concentration of product (P), normalized to ribozyme concentration (R), is plotted versus time for hammerheads 6 (*A*) and 8 (*B*) in reactions with 4 nM ribozyme and 200 nM substrate, for hammerhead 9 (*C*) in a reaction with 100 nM ribozyme and 2000 nM substrate, and for hammerhead 10 (*D*) in a reaction with 200 nM ribozyme and 10,000 nM substrate.

Steady-state cleavage velocities were measured for each hammerhead at several substrate concentrations that were at least 10-fold greater than ribozyme concentrations (Fig. 3). Cleavage rates were first order in substrate concentration at low concentrations, and the ribozymes were effectively saturated with substrate at high concentrations, indicating that hammerhead kinetics are amenable to analysis using the Michaelis–Menten rate equation. Michaelis–Menten parameters for each hammerhead sequence are shown in Table 1. Values of k_{cat} are similar, but K_m values differ nearly 60-fold, with a particularly high K_m characteristic of hammerhead 10.

In addition to the high K_m found for hammerhead 10, this hammerhead displays unusual cleavage properties in several other respects. When reactions are allowed to proceed to completion, hammerhead 10 differs markedly from the others in the maximum extent of cleavage. Whereas most of substrates 6, 8, and 9 can be cleaved, only 40% of substrate 10 is converted to product (Fig. 4). The same extent of cleavage is found for substrate concentrations ranging from 0.5 μM to 8 μM, so it is not a consequence of equilibrium between foward and reverse reactions. Reactions containing more ribozyme than substrate proceed to the same limited extent, so product inhibition or decay of ribozyme activity with time do not account for the data.

One possible explanation for the limited cleavage of substrate 10 was that a portion of this substrate was chemically different from the cleavable fraction, due perhaps to misincorporation of critical nucleotides during transcription. To

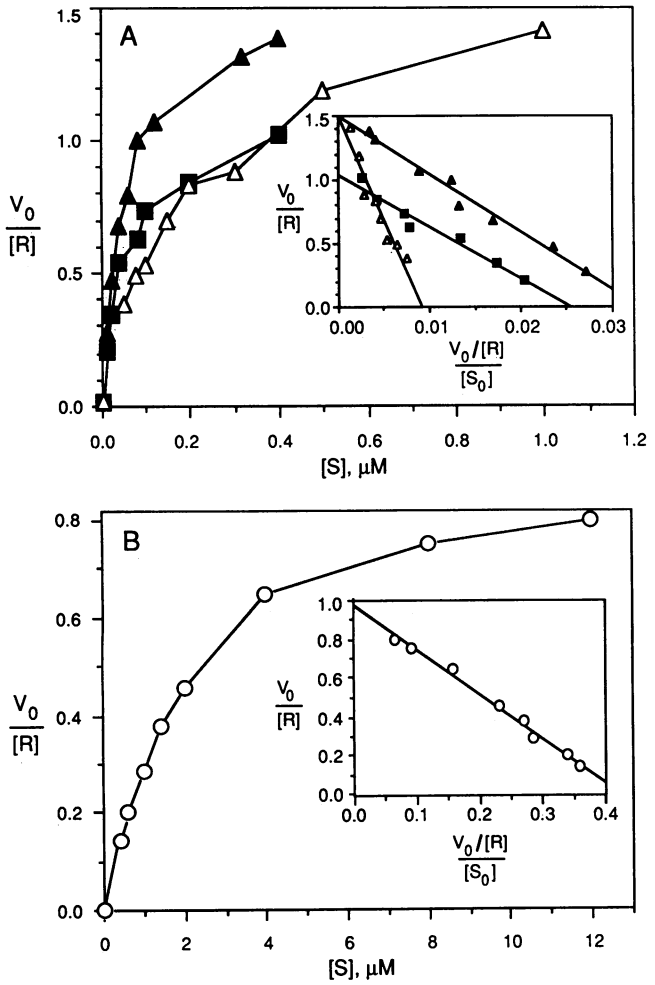

FIG. 3. Steady-state kinetics of hammerhead cleavage reactions. (*A*) The steady-state rate of cleavage (V_0, nM·min^{-1}) normalized to ribozyme (R) concentration is plotted versus substrate (S) concentration for hammerheads 6 (▲), 8 (■), and 9 (△). Ribozyme concentrations were 1 nM for hammerheads 6 and 8 and 5 nM for hammerhead 9. (*Inset*) Eadie–Hofstee plots of these data. (*B*) The steady-state rate of cleavage (V_0, nM·min^{-1}) normalized to the ribozyme concentration of 50 nM is plotted versus substrate concentration for hammerhead 10. (*Inset*) Eadie–Hofstee plot of these data.

test this possibility, a large scale reaction was allowed to proceed to completion. The uncut substrate was purified from a denaturing gel and incubated with ribozyme again under the original conditions. The repurified fraction was found to undergo cleavage at virtually the same initial rate and to the same extent as the original substrate (Fig. 4). Since cleavable substrate can be generated from the uncut portion by repurification, the feature that distinguishes the uncut fraction is conformational rather than chemical.

To assess the structural homogeneity of the substrate RNAs, their electrophoretic behavior was examined in the presence of magnesium under conditions similar to those used for cleavage reactions (Fig. 5*A*). The two substrates for reactions having the lowest K_m values, substrates 6 and 8, migrate as single species over a range of concentration of

Table 1. Michaelis–Menten parameters for hammerhead cleavage

Hammerhead	K_m, nM	k_{cat}, min^{-1}	k_{cat}/K_m, nM^{-1}·min^{-1}
6	46	1.5	0.032
8	41	1.0	0.024
9	160	1.5	0.0093
10	2300	1.0	0.00044

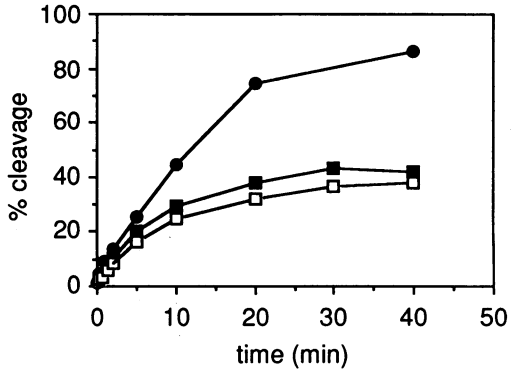

FIG. 4. Time course of cleavage. The fraction of substrate converted to product at various times is shown for hammerhead 6 (●) in a reaction containing 10 nM ribozyme and 250 nM substrate and for hammerhead 10 (■) in a reaction containing 100 nM ribozyme and 3000 nM substrate. The third line (□) represents cleavage of repurified substrate 10 that was left intact at the end of the first cleavage time course.

2–10,000 nM. Substrate 9, with an intermediate K_m value, migrates as one species containing ≈90% of the total material and three minor species with lower electrophoresis mobilities. Substrate 10, with the highest K_m value, also migrates heterogeneously with three major and two minor species. The most intense band comprises 40% of the total material and migrates most rapidly. Relative amounts of some species of substrates 9 and 10 change with concentration, suggesting that they are aggregates.

To demonstrate that the more slowly migrating species of substrates 9 and 10 are multimolecular, we examined the electrophoretic mobility of 5′-^{32}P-labeled RNA after renaturing with a large excess of nonradiolabeled RNA having 5′ triphosphate termini (data not shown). Since the electrophoretic mobility of RNA having 5′ triphosphate termini is slower on nondenaturing gels than that of RNA having 5′ monophosphate termini, a complex containing RNAs with different termini would migrate slower than homogeneous 5′-^{32}P-labeled RNA. By this criterion, all of the slower migrating species are multimeric complexes, whereas the most rapidly migrating species are unimolecular.

Only the fast-mobility monomeric species is depleted during a time course of cleavage (Fig. 5*B*). The incomplete cleavage shown in Fig. 4 is therefore explained by the fact that the aggregates are cleavage-resistant. We have found that, in the presence of magnesium, these inactive aggregates do not equilibrate with the cleavable monomer over a period of days. After being eluted from a nondenaturing gel and precipitated with ethanol, they remain resistant to cleavage and retain their characteristic mobility during subsequent electrophoresis. Only heating to 95°C in the presence of EDTA or purification on a denaturing gel (Fig. 4) disrupts the aggregates enough to produce a significant fraction of cleavable monomers.

The high K_m observed for hammerhead 10 cannot be attributed solely to the presence of aggregates. If the fraction of inactive substrate is taken into account, the K_m value can be adjusted by 60%, to 920 nM. This value is still nearly 20-fold greater than the K_m values observed for hammerheads 6 and 8. The presence of a partial palindrome in the sequence of substrate 10 suggests an explanation for both its high K_m value and its tendency to aggregate. As shown in Fig. 5*C*, this RNA can form a hairpin with at least three base pairs as well as aggregates with even more intermolecular base pairs. No structures with comparable stabilities can be inferred from the other substrate sequences. Since a hairpin must be disrupted to assemble the hammerhead, a higher concentration of substrate would be required to drive assembly. A

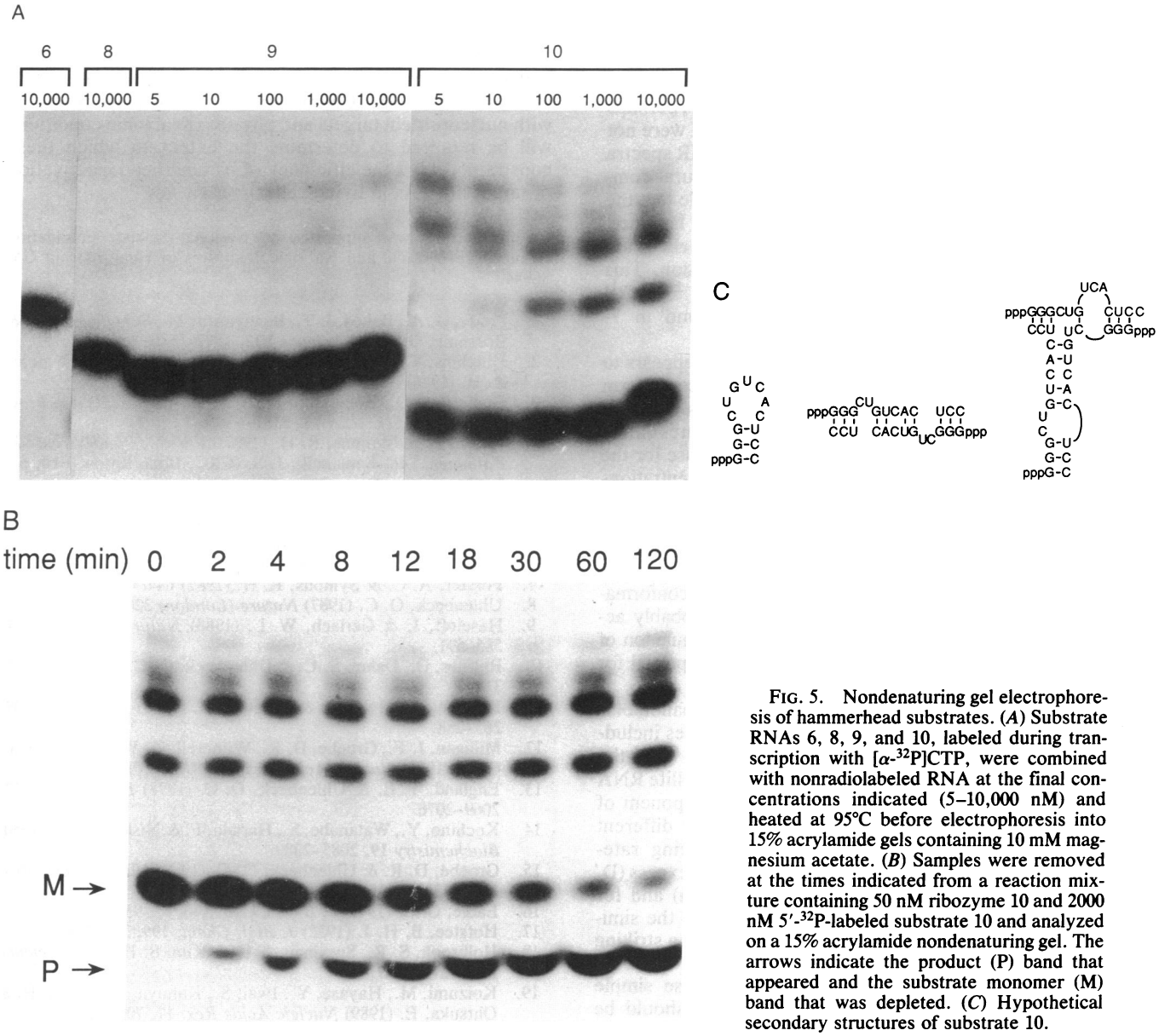

FIG. 5. Nondenaturing gel electrophoresis of hammerhead substrates. (*A*) Substrate RNAs 6, 8, 9, and 10, labeled during transcription with [α-^{32}P]CTP, were combined with nonradiolabeled RNA at the final concentrations indicated (5–10,000 nM) and heated at 95°C before electrophoresis into 15% acrylamide gels containing 10 mM magnesium acetate. (*B*) Samples were removed at the times indicated from a reaction mixture containing 50 nM ribozyme 10 and 2000 nM 5′-^{32}P-labeled substrate 10 and analyzed on a 15% acrylamide nondenaturing gel. The arrows indicate the product (P) band that appeared and the substrate monomer (M) band that was depleted. (*C*) Hypothetical secondary structures of substrate 10.

greater potential for hydrogen bonding in the aggregates, relative to the hairpin, could account for their greater stability and resistance to cleavage.

In the light of this evidence regarding the structural heterogeneity of hammerhead substrate RNAs, we were curious about the behavior of ribozymes on nondenaturing gels. When the four ribozymes are subjected to gel electrophoresis under nondenaturing conditions, they all migrate as single species at the concentrations used for kinetic analyses. At concentrations of ribozyme 6 above 100 nM, however, multiple species of lower mobility were observed, suggesting aggregation. Alternate conformations of ribozyme RNAs probably contribute little to variation in cleavage kinetics since they are structurally homogeneous at the concentrations used for kinetic analyses.

DISCUSSION

Seventy-fold differences in cleavage rates have been reported among hammerhead sequences that contain identical nucleotides at the active site but differ in the base composition of the helices generated by the binding of the substrate to the ribozyme (10). Comparison of steady-state kinetics among four such sequences indicates that the differences in catalytic efficiency are due entirely to differences in K_m values. By assuming a simple reaction mechanism consisting of substrate binding, cleavage, and product release, the similarity in k_{cat} values could indicate that cleavage chemistry is rate-determining. The other steps in this simple mechanism are less likely to be rate-determining. Since reaction rates during the first substrate turnover change little during subsequent turnovers, product dissociation is not significantly slower than earlier steps in the reaction. Hammerhead assembly may consist solely of substrate binding, which, of course, will not be rate-limiting at saturating concentrations. Assembly may be more complex than simple binding, however. It is possible that the two intermolecular helices on either side of the cleavage site form at different rates. One helix may form quickly, in a bimolecular reaction; formation of the second helix may require a slow conformational change. Further kinetic and structural data will reveal whether this or some other additional step is involved in the reaction mechanism.

The similarity in k_{cat} values among these hammerheads strongly supports the view that all the critical components for cleavage lie in the central core of the domain consisting of nine non-base-paired nucleotides and the pair adjacent to the cleavage site. Although different helix sequences could po-

tentially alter active site geometry indirectly through altered stacking (18), this effect appears to be small, perhaps accounting for the <2-fold differences in k_{cat} values. An alternative explanation for the slight variation in k_{cat} values is that the specific activities of the ribozymes differ slightly, perhaps due to the presence of inactive conformations that were not detected by nondenaturing gel electrophoresis. NMR spectra have shown considerable differences in the structural complexity of several ribozymes (26). It is quite possible that the rate-determining step will be different for different hammerhead sequences. Hammerheads with more stable helices are likely to be limited by rates of product dissociation. This would explain much lower values of k_{cat} ($\approx 10^{-2}$ min^{-1}) reported for hammerheads with products bound in 7-base-pair helices (19).

The variation in K_m values among hammerheads appears to result from the propensity of some substrate sequences to form structures that are incompatible with hammerhead assembly. If these structures can equilibrate with cleavable structures during the course of the reaction, as appeared to be the case for the monomeric conformation of substrate 10, high concentrations of RNA will be required to drive complex formation, resulting in a correspondingly high K_m for the reaction. Some structures of substrate 10 were so stable that they failed to exchange into cleavable substrates on the time scale of the reaction and were essentially inert. The ability of RNA to adopt stable conformations incompatible with hammerhead assembly probably accounts for the low extents of cleavage and the stimulation of cleavage by heating and cooling that have been reported for several hammerhead sequences (20).

Values of k_{cat} of ≈ 1 min^{-1} and K_m values in the nanomolar range are characteristic of most RNA endonucleases including the *Tetrahymena* intervening sequence (IVS) (21), the hairpin catalytic domain of the negative-strand satellite RNA of tobacco ringspot virus (22), and the RNA component of RNase P (23). Because these reactions occur by different mechanisms (24), with product dissociation being rate-determining for the IVS reaction in RNA substrate excess (D. Herschlag and T. Cech, personal communication) and for RNA-catalyzed cleavage of precursor tRNA (25), the similarity in catalytic efficiency may be little more than a striking coincidence.

Kinetic and structural characterization of these simple hammerheads point to two considerations that should be relevant to the design of ribozymes as endonucleases directed against specific target mRNAs. First, helix length and base composition will probably determine how well a particular ribozyme will function catalytically under physiological conditions. If very stable helices are generated in the binding of the ribozyme to the target RNA, the rate of product dissociation will decrease to become rate limiting and perhaps slow enough to prevent multiple turnover. The second factor contributing to catalytic efficiency is the secondary structure of the target RNA. Sequestering of the target sequence in a stable secondary structure that is incompatible with hammerhead domain assembly can greatly increase the concentrations required to achieve maximum cleavage rates. At worst, stable target structures may fail to assemble into the hammerhead domain altogether and may remain completely resistant to cleavage. Characterization of cleavage reactions with nucleoprotein targets and physiological ionic conditions will be required to determine the extent to which these constraints affect the efficiency of hammerhead inactivation of target mRNAs in living cells.

This research was supported by National Science Foundation Grant DMB-8805690 and National Institutes of Health Grant GM 36944.

1. Prody, G. A., Bakos, J. T., Buzayan, J. M., Schneider, I. R. & Bruening, G. (1986) *Science* **232**, 1577–1580.
2. Hutchins, C. J., Rathjen, P. D., Forster, A. C. & Symons, R. H. (1986) *Nucleic Acids Res.* **14**, 3627–3640.
3. Branch, A. D., Robertson, H. D. & Dickson, E. (1981) *Proc. Natl. Acad. Sci. USA* **78**, 6381–6385.
4. Keese, P. & Symons, R. H. (1987) in *Viroids and Viroid-like Pathogens*, ed. Semancik, J. S. (CRC, Boca Raton, FL), pp. 1–47.
5. Buzayan, J. M., Gerlach, W. L. & Bruening, G. (1986) *Nature (London)* **323**, 349–353.
6. Buzayan, J. M., Gerlach, W. L. & Bruening, G. (1986) *Proc. Natl. Acad. Sci. USA* **83**, 8859–8862.
7. Forster, A. C. & Symons, R. H. (1987) *Cell* **49**, 211–220.
8. Uhlenbeck, O. C. (1987) *Nature (London)* **328**, 596–600.
9. Haseloff, J. & Gerlach, W. L. (1988) *Nature (London)* **334**, 585–591.
10. Ruffner, D., Dahm, S. C. & Uhlenbeck, O. C. (1989) *Gene* **82**, 31–41.
11. Koizumi, M., Iwai, S. & Ohtsuka, E. (1988) *FEBS Lett.* **239**, 285–288.
12. Milligan, J. F., Groebe, D. R., Witherell, G. W. & Uhlenbeck, O. C. (1987) *Nucleic Acids Res.* **15**, 8783–8798.
13. England, T. E. & Uhlenbeck, O. C. (1978) *Biochemistry* **17**, 2069–2076.
14. Kochino, Y., Watanabe, S., Harada, F. & Nishimura, S. (1980) *Biochemistry* **19**, 2085–2089.
15. Groebe, D. R. & Uhlenbeck, O. C. (1988) *Nucleic Acids Res.* **16**, 11725–11735.
16. Eadie, G. S. (1942) *J. Biol. Chem.* **146**, 85–93.
17. Hofstee, B. H. J. (1952) *J. Biol. Chem.* **199**, 357–364.
18. Holbrook, S. R., Sussman, J. L. & Kim, S.-H. (1981) *Science* **212**, 1275–1277.
19. Koizumi, M., Hayase, Y., Iwai, S., Kamiya, H., Inoue, H. & Ohtsuka, E. (1989) *Nucleic Acids Res.* **17**, 7059–7071.
20. Sheldon, C. C. & Symons, R. H. (1989) *Nucleic Acids Res.* **17**, 5665–5677.
21. Zaug, A. J., Grosshans, C. A. & Cech, T. R. (1988) *Biochemistry* **27**, 8924–8931.
22. Hampel, A. & Tritz, R. (1989) *Biochemistry* **28**, 4929–4933.
23. Guerrier-Takada, C., Gardiner, K., Marsh, T., Pace, N. & Altman, S. (1983) *Cell* **35**, 849–857.
24. Cech, T. R. (1987) *Science* **236**, 1532–1539.
25. Reich, C., Olsen, G. J., Pace, B. & Pace, N. R. (1988) *Science* **239**, 178–183.
26. Heus, H. A., Uhlenbeck, O. C. & Pardi, A. (1990) *Nucleic Acids Res.*, in press.